Proline dehydrogenase promotes senescence through the generation of reactive oxygen species

Nagano, Taiki ; Nakashima, Akio ; Onishi, Kengo ; Kawai, Kosuke ; Awai, Yuto ; Kinugasa, Mizuki ; Iwasaki, Tetsushi ; Kikkawa, Ushio ; Kamada,…

(Citation)
Journal of Cell Science,130(8):1413-1420

(Issue Date)
2017-04-15

(Resource Type)
journal article

(Version)
Version of Record

© 2017. Published by The Company of Biologists Ltd | Journal of Cell Science (2017) 130, 1413-1420 doi:10.1242/jcs.196469

RESEARCH ARTICLE

Proline dehydrogenase promotes senescence through the generation of reactive oxygen species

Taiki Nagano[1,2], Akio Nakashima[3,4], Kengo Onishi[2], Kosuke Kawai[2], Yuto Awai[5], Mizuki Kinugasa[5], Tetsushi Iwasaki[1,2,5], Ushio Kikkawa[3,4] and Shinji Kamada[1,2,5,*]

ABSTRACT

Cellular senescence is a complex stress response characterized by permanent loss of proliferative capacity and is implicated in age-related disorders. Although the transcriptional activity of p53 (encoded by *TP53*) is known to be vital for senescence induction, the downstream effector genes critical for senescence remain unsolved. Recently, we have identified the proline dehydrogenase gene (*PRODH*) to be upregulated specifically in senescent cells in a p53-dependent manner, and the functional relevance of this to senescence is yet to be defined. Here, we conducted functional analyses to explore the relationship between PRODH and the senescence program. We found that genetic and pharmacological inhibition of PRODH suppressed senescent phenotypes induced by DNA damage. Furthermore, ectopic expression of wild-type PRODH, but not enzymatically inactive forms, induced senescence associated with the increase in reactive oxygen species (ROS) and the accumulation of DNA damage. Treatment with N-acetyl-L-cysteine, a ROS scavenger, prevented senescence induced by PRODH overexpression. These results indicate that PRODH plays a causative role in DNA damage-induced senescence through the enzymatic generation of ROS.

KEY WORDS: Amino acid metabolism, p53, PRODH, Reactive oxygen species, Senescence

INTRODUCTION

Cellular senescence is defined as a state of irreversible growth arrest induced by genotoxic stresses, including DNA-damaging agents and reactive oxygen species (ROS), and is implicated in both tumor suppression and age-related diseases (d'Adda di Fagagna, 2008; Kuilman et al., 2010; Campisi, 2013; Salama et al., 2014; Serrano et al., 1997; Chen and Ames, 1994; Di Leonardo et al., 1994). In response to genotoxic stresses, DNA damage response (DDR) signaling activates p53 (encoded by *TP53*), a transcription factor that is essential for the initiation and maintenance of senescence (Vousden and Prives, 2009; Rufini et al., 2013). Activated p53 induces the expression of genes involved in senescence, such as those encoding p21 (*CDKN1A*) and E2F7 (el-Deiry et al., 1993; Aksoy et al., 2012; Carvajal et al., 2012). Although p21 is well known to play a critical role in the cell cycle arrest of senescent cells (Romanov et al., 2012; Noda et al., 1994), the complete set of p53 target genes required for the senescence program remains to be elucidated (Brady et al., 2011; Valente et al., 2013).

We have recently revealed, by comparing the transcriptome between senescent and apoptotic cells, that the proline dehydrogenase gene (*PRODH*) is upregulated specifically in senescent cells and that p53 binds to and activates *PRODH* in response to senescence-inducing DNA damage (Nagano et al., 2016). PRODH is a mitochondrial inner membrane-associated enzyme catalyzing the first and rate-limiting step in proline catabolism, forming Δ^1-pyrroline-5-carboxylic acid (P5C), and notably ROS are generated as byproducts of the reaction (Phang et al., 2008). It has been reported that PRODH is transcriptionally activated by p53 in response to genotoxic insults and, consistent with its enzymatic function, upregulation of PRODH leads to intracellular ROS accumulation and ultimately to apoptotic cell death (Polyak et al., 1997; Raimondi et al., 2013; Donald et al., 2001; Hu et al., 2007). However, ROS and the resulting oxidative damage to DNA can induce senescence as well as apoptosis (Chen and Ames, 1994; te Poele et al., 2002; Walker et al., 1991), and our previous results obtained from comparative transcriptomic analyses suggest that PRODH can preferentially function in senescence rather than apoptosis. Although we have observed that overexpression of PRODH in normal and tumor cells induces senescent phenotypes, such as loss of proliferative capacity and the expression of senescence-associated β-galactosidase (SA-β-Gal; encoded by *GLB1*) (Nagano et al., 2016), whether and how PRODH functionally contributes to the senescence program remains uncertain.

In the present study, we explored the functional relationship between PRODH and senescence. We reveal that genetic and pharmacological inhibition of PRODH impairs DNA damage-induced senescence and that overexpression of PRODH induces intracellular ROS accumulation and DNA damage.

RESULTS

Genetic and pharmacological inhibition of PRODH impairs DNA damage-induced senescence

To test the importance of PRODH in DNA damage-induced senescence, we examined the effect of *PRODH* knockdown in a human osteosarcoma cell line (U2OS) expressing wild-type (WT) p53 (Fig. 1A). The cells that had been transfected with an siRNA pool against *PRODH*, comprising four different oligonucleotides, were treated with etoposide, an anticancer drug that causes DNA double-strand breaks, and the extent of senescence was determined by examining well-established senescence markers – staining of SA-β-Gal (Dimri et al., 1995) and loss of proliferative capacity. We

[1]Division of Signal Pathways, Biosignal Research Center, Kobe University, 1-1 Rokkodai-cho, Nada-ku, Kobe 657-8501, Japan. [2]Department of Biology, Graduate School of Science, Kobe University, 1-1 Rokkodai-cho, Nada-ku, Kobe 657-8501, Japan. [3]Division of Signal Functions, Biosignal Research Center, Kobe University, 1-1 Rokkodai-cho, Nada-ku, Kobe 657-8501, Japan. [4]Department of Bioresource Science, Graduate School of Agricultural Science, Kobe University, 1-1 Rokkodai-cho, Nada-ku, Kobe 657-8501, Japan. [5]Department of Biology, Faculty of Science, Kobe University, 1-1 Rokkodai-cho, Nada-ku, Kobe 657-8501, Japan.

*Author for correspondence (skamada@kobe-u.ac.jp)

S.K., 0000-0003-0658-1785

Received 8 August 2016; Accepted 23 February 2017

Journal of Cell Science (2017) 130, 1413-1420 doi:10.1242/jcs.196469

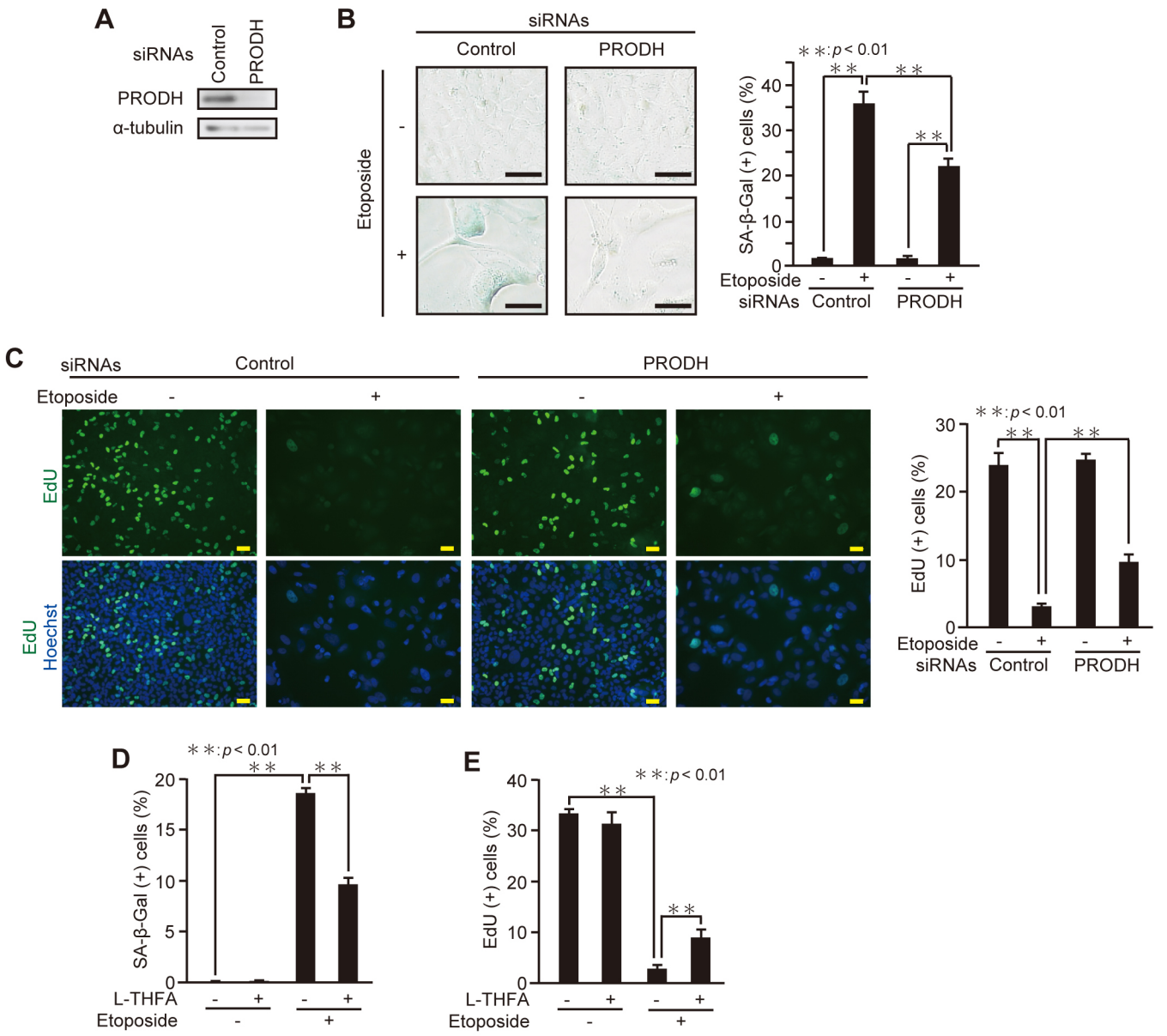

Fig. 1. Genetic and pharmacological inhibition of PRODH impairs DNA damage-induced senescence in U2OS cells. (A) U2OS cells transfected with siRNA against *PRODH* were treated with 2 µM etoposide for 5 days and subjected to immunoblot analysis. (B) *PRODH*-depleted U2OS cells that had been treated with 2 µM etoposide for 7 days were subjected to staining for SA-β-Gal. Representative images (left) and the percentage of SA-β-Gal-positive cells (right) are shown. Scale bars: 50 µm. (C) *PRODH*-depleted cells treated with 2 µM etoposide for 7 days were subjected to an EdU proliferation assay. Representative images (left) and the percentage of EdU-positive cells (right) are shown. Scale bars: 50 µm. (D,E) U2OS cells treated with 2 µM etoposide and 5 mM L-THFA for 7 days were subjected to staining of SA-β-Gal (D) and an EdU proliferation assay (E). Data are mean±s.d. Statistical significance was determined using the Student's *t*-test analysis (*n*=3 independent cultures); ***P*<0.01.

observed that a sublethal dose of etoposide (2 µM) effectively induced the expression of SA-β-Gal activity in U2OS cells as reported previously (Nakano et al., 2013) and, more importantly, knockdown of *PRODH* impaired the etoposide-induced SA-β-Gal activation (Fig. 1B). To test whether *PRODH* depletion reverses etoposide-induced loss of proliferation capacity, we examined the growth of etoposide-treated U2OS cells with a 5-ethynyl-2′-deoxyuridine (EdU) incorporation assay (Fig. 1C). Consistent with the decrease in SA-β-Gal activity, loss of proliferative capacity induced by etoposide was partially reversed by *PRODH* depletion. These results suggest that PRODH is positively involved in the regulation of senescence. To confirm this, we next tested the impact of inhibiting PRODH activity on senescence using L-tetrahydro-2-furoic acid (L-THFA), previously identified and characterized for the ability to inhibit the enzymatic activity of PRODH (Tallarita et al., 2012). L-THFA effectively suppressed senescence caused by etoposide treatment (Fig. 1D). Consistently, the DNA damage-induced loss of proliferative capacity was partly reversed by L-THFA (Fig. 1E), supporting the idea that PRODH contributes to senescence induction. To test whether the role of PRODH in senescence is conserved in untransformed cells, we included normal human fibroblast Hs68 cells in the analyses. As is the case in U2OS cells, a low dose of etoposide (0.5 µM) led Hs68 cells to undergo senescence in a time-dependent manner, as judged by the activation of SA-β-Gal (Fig. 2A). Furthermore, knockdown of *PRODH* impaired etoposide-induced SA-β-Gal activation in Hs68 cells as in

Journal of Cell Science (2017) 130, 1413-1420 doi:10.1242/jcs.196469

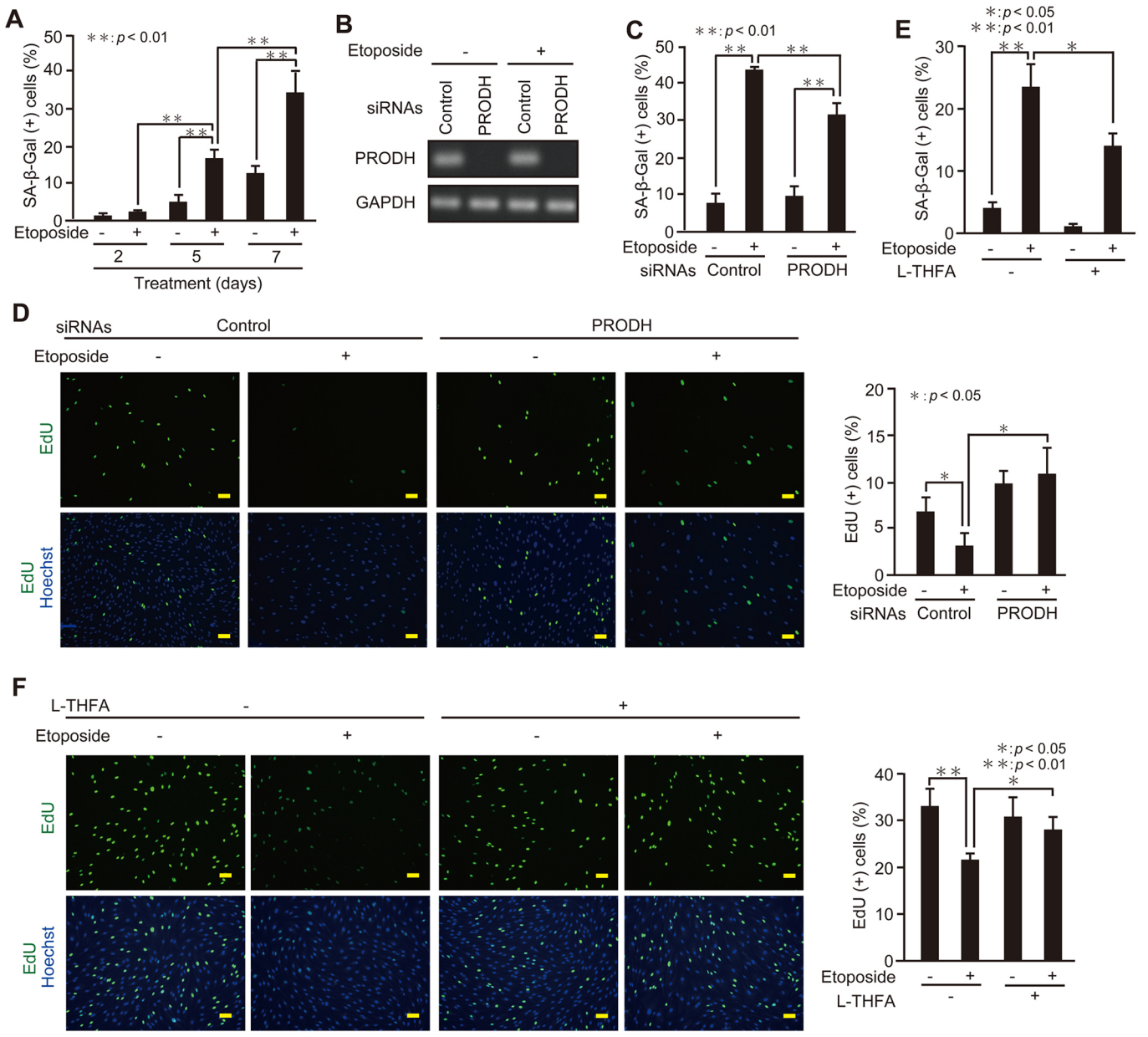

Fig. 2. Inhibition of PRODH impairs DNA damage-induced senescence in normal human fibroblast Hs68 cells. (A) Hs68 cells treated with 0.5 µM etoposide for the indicated times were subjected to staining of SA-β-Gal. (B) Hs68 cells transfected with siRNA against *PRODH* were treated with 0.5 µM etoposide for 5 days, and the expression levels of *PRODH* were analyzed by semi-quantitative RT-PCR. (C,D) *PRODH*-depleted Hs68 cells treated with 0.5 µM etoposide for 7 days were subjected to staining of SA-β-Gal (C) and an EdU proliferation assay (D). (D) Representative images (left) and the percentage of EdU-positive cells (right) are shown. Scale bars: 100 µm. (E,F) Hs68 cells treated with 0.5 µM etoposide and 5 mM L-THFA for 7 days were subjected to staining of SA-β-Gal (E) and an EdU proliferation assay (F). (F) Representative images (left) and the percentage of EdU-positive cells (right) are shown. Scale bars: 100 µm. Data are mean±s.d. Statistical significance was determined using the Student's *t*-test analysis (n=3 independent cultures).

U2OS cells (Fig. 2B,C). In line with this, knockdown of *PRODH* reversed the etoposide-induced loss of proliferation capacity (Fig. 2D). In addition, pharmacological inhibition of PRODH with L-THFA also inhibited etoposide-induced senescence in Hs68 cells, as determined using SA-β-Gal and EdU proliferation assays (Fig. 2E,F). These results indicate that PRODH promotes senescence in both tumor and normal cells.

PRODH induces senescence via ROS production

We next set out to determine the mechanism by which PRODH promotes senescence. Since PRODH is known to produce ROS as a byproduct of proline oxidation (Donald et al., 2001), and ROS induce senescence through oxidative damage (Campisi, 2013; Salama et al., 2014; Lu and Finkel, 2008), we first examined whether overexpression of PRODH results in ROS accumulation. In accordance with our previous results (Nagano et al., 2016), ectopic expression of PRODH modestly induced senescence in U2OS cells, as judged using SA-β-Gal and EdU assays (Fig. 3A-C). Furthermore, addition of the PRODH substrate, proline, to the medium enhanced the SA-β-Gal activation induced by PRODH overexpression in a dose-dependent manner (Fig. 3D), which suggests that PRODH induces senescence through its enzymatic activity. Moreover, ectopic PRODH expression did not induce apoptosis in this setting (Fig. 3E), confirming the preferential role of

Journal of Cell Science (2017) 130, 1413-1420 doi:10.1242/jcs.196469

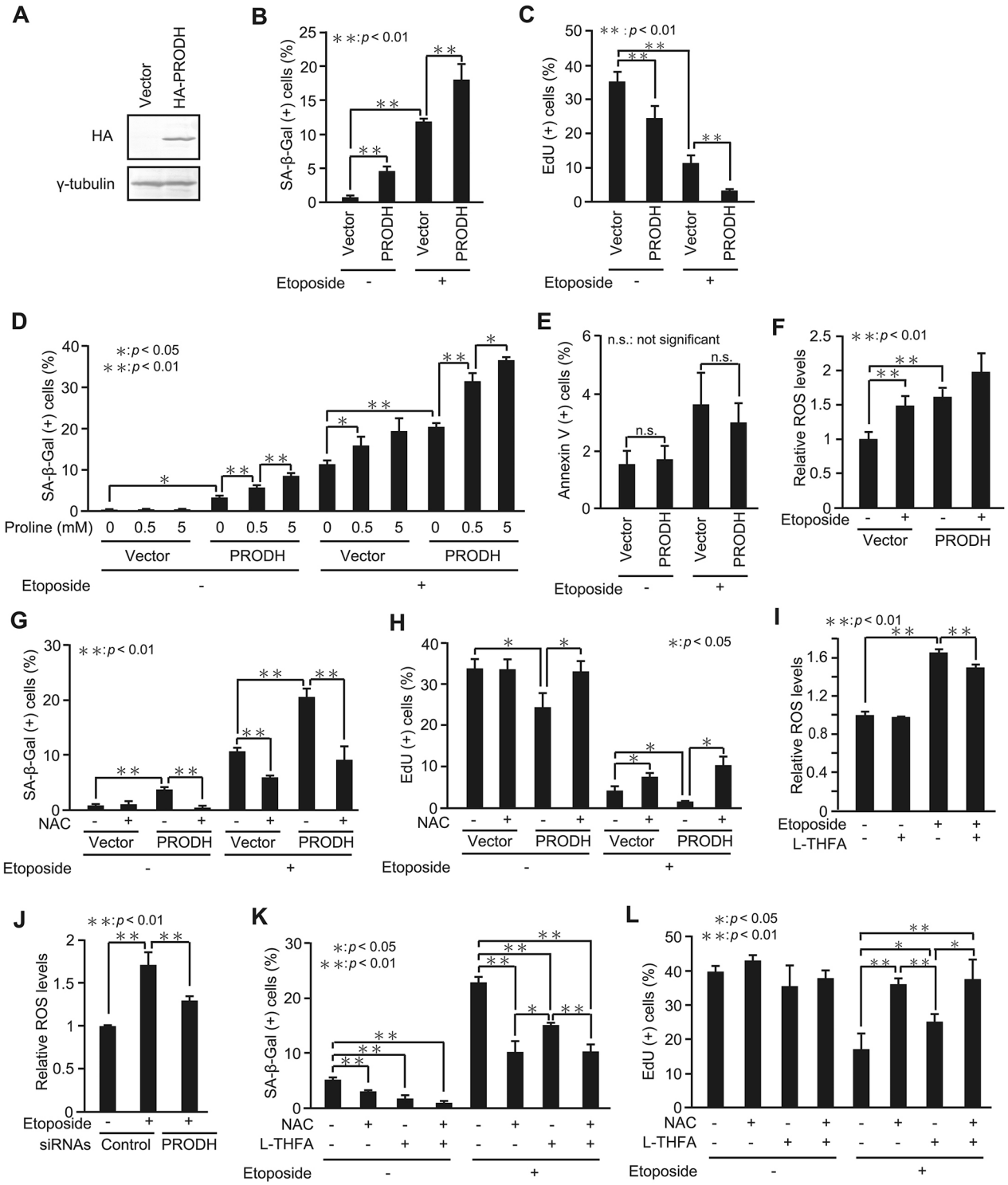

Fig. 3. PRODH induces senescence via ROS production. (A) U2OS cells transfected with pcDNA3-HA encoding WT PRODH were subjected to immunoblot analysis. (B,C) PRODH-overexpressing U2OS cells selected with G418 and treated with 2 µM etoposide for 7 days were subjected to staining of SA-β-Gal (B) and an EdU proliferation assay (C). (D) PRODH-overexpressing U2OS cells selected with G418 and treated with 2 µM etoposide for 7 days in DMEM supplemented with the indicated concentrations of proline were subjected to staining of SA-β-Gal. Proline was not present in the base DMEM. (E) PRODH-overexpressing U2OS cells treated with 2 µM etoposide for 7 days were subjected to Annexin V staining. (F) PRODH-overexpressing U2OS cells were treated with 2 µM etoposide for 30 h, and ROS levels were measured using the ROS-Glo H_2O_2 Assay kit. (G,H) U2OS cells transfected with pcDNA3-HA encoding WT PRODH were selected with G418 and treated with 2 µM etoposide in the presence of 5 mM NAC. After incubation for 7 days, the cells were subjected to staining for SA-β-Gal (G) and an EdU proliferation assay (H). (I) U2OS cells treated with 2 µM etoposide and 5 mM L-THFA were subjected to a ROS assay using the ROS-Glo H_2O_2 Assay kit. (J) U2OS cells depleted of PRODH were treated with 2 µM etoposide for 30 h, and ROS levels were measured with a different ROS-sensitive dye, CM-H_2DCFDA. (K,L) Hs68 cells treated with 0.5 µM etoposide for 7 days in the presence of 5 mM NAC and/or 5 mM L-THFA as indicated were subjected to staining for SA-β-Gal (K) and an EdU proliferation assay (L). Data are mean±s.d. Statistical significance was determined using the Student's *t*-test analysis (n=3 independent cultures). n.s., not significant (P>0.05).

Journal of Cell Science

Journal of Cell Science (2017) 130, 1413-1420 doi:10.1242/jcs.196469

PRODH to induce senescence rather than apoptosis. To measure ROS levels, we used a luminescent ROS-Glo H_2O_2 assay kit that detects H_2O_2 in cell culture. Intracellular ROS levels were elevated in the cells that overexpressed PRODH compared with those in empty vector-transfected cells (Fig. 3F). The difference in ROS levels was not large but likely to be sufficient to promote the senescence program as the ROS levels of PRODH-overexpressing cells were comparable to those of etoposide-induced senescent cells (compare second and third bars in Fig. 3F). In addition, treatment with N-acetyl-L-cysteine (NAC), a potent ROS scavenger, markedly suppressed senescence induced by PRODH overexpression (Fig. 3G,H), suggesting that induction of senescence by ectopic PRODH expression occurred via the generation of ROS. Consistently, the increase in ROS production upon etoposide treatment was partially suppressed by co-treating with L-THFA (Fig. 3I). The contribution of PRODH to ROS accumulation was further confirmed by using another ROS-sensitive dye, CM-H_2DCFDA (Fig. 3J). Knockdown of PRODH impaired the etoposide-induced ROS accumulation. To further test whether the function of PRODH in senescence could be explained solely by ROS generation, we compared the effect of NAC and L-THFA on suppressing senescence in Hs68 cells. We found that both NAC and L-THFA also impaired etoposide-induced senescence in Hs68 cells, and combined treatment with NAC and L-THFA had no additive effect compared to single treatment with NAC (Fig. 3K,L), suggesting that the effect of PRODH on promoting senescence is fully dependent on ROS production. It should be noted here that inhibition of PRODH did not completely prevent DNA damage-induced senescence and ROS production (Figs 1B-E, 2C,E and 3I,J), and NAC was more effective in inhibiting senescence than L-THFA (Fig. 3K,L). These results suggest that ROS accumulation during senescence is dependent not only on PRODH but also on other redox regulatory mechanism(s), and PRODH contributes to increase the intracellular ROS level beyond a threshold to trigger senescence.

Enzymatically inactive forms of PRODH fail to induce ROS accumulation and senescence

To further confirm that the effect of PRODH on senescence induction is due to its enzymatic activity, we have generated two PRODH mutants, each with a single point mutation (L441P and R453C), and both have been shown to have little enzymatic activity (<10% activity of WT) *in vitro* (Bender et al., 2005), as confirmed here by the inability to increase intracellular ROS levels, as compared to WT PRODH (Fig. 4A,B). Unlike WT PRODH, both mutants were unable to promote senescence, both in the absence and presence of etoposide (Fig. 4C,D), which further supports the idea that PRODH induces senescence via enzymatic ROS production.

PRODH overexpression causes DNA damage

ROS can cause DNA damage, and DDR signaling is an important initiator and sustainer of the senescent state. Given the role of PRODH in ROS production, we next tested whether PRODH overexpression induces DNA damage. For this purpose, we monitored DNA double-strand breaks using well-established markers, phosphorylated histone H2AX (γH2AX) and 53BP1. Upon DNA breakage, H2AX is phosphorylated by ATM, and foci of γH2AX and 53BP1 are formed at the double-strand break sites (Rogakou et al., 1999; Schultz et al., 2000). Mitochondrial localization of hemagglutinin (HA)-tagged PRODH was confirmed using the mitochondria-specific fluorescent dye, MitoTracker (Fig. 5A), indicating that the HA-tag does not affect the subcellular localization of PRODH. U2OS cells transiently overexpressing HA-tagged PRODH constructs (WT, L441P and R453C) were immunostained with antibodies against γH2AX and 53BP1, in combination with an antibody against HA (Fig. 5B,C). The cells overexpressing WT PRODH exhibited an increased number of γH2AX and 53BP1 foci as compared with the cells that expressed the PRODH mutants, suggesting that the enzymatic activity of PRODH facilitates DNA damage. Overall, these results show that, upon treatment with a sublethal dose of etoposide, p53-mediated upregulation of PRODH leads to ROS accumulation, which ultimately establishes senescence.

DISCUSSION

PRODH is a p53-inducible gene as a result of its intronic p53 responsive elements (Polyak et al., 1997; Raimondi et al., 2013; Nagano et al., 2016), and upregulation of PRODH results in the formation of proline-dependent ROS (Donald et al., 2001). Although PRODH has been suggested to play a role in p53-induced apoptosis (Polyak et al., 1997; Hu et al., 2007), our results clearly show that PRODH is a crucial molecule in DNA damage-induced senescence. We revealed that overexpression of wild-type PRODH, but not of enzymatically inactive forms, induce senescence, and that genetic and pharmacological inhibition of PRODH suppresses DNA damage-induced senescence. Moreover, ectopic expression of PRODH increased intracellular ROS levels,

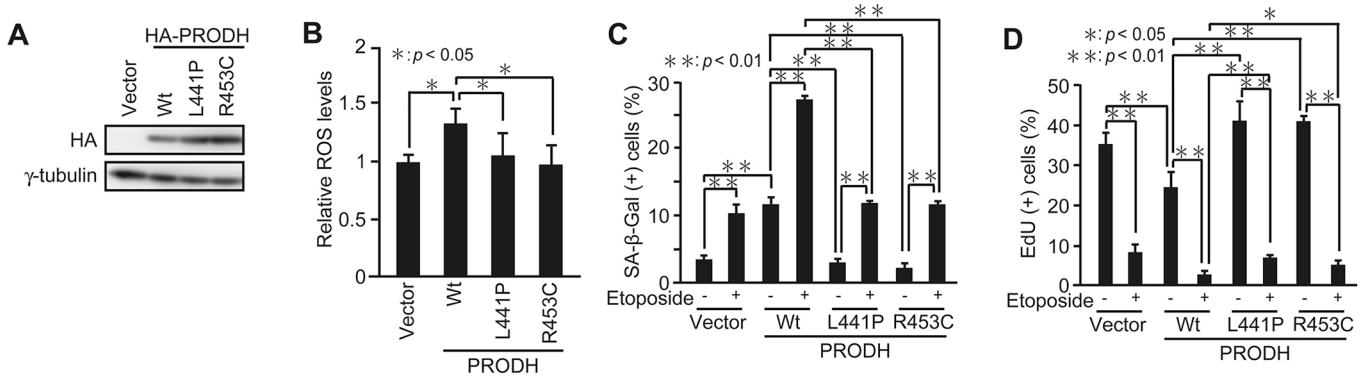

Fig. 4. Enzymatically inactive forms of PRODH fails to induce ROS accumulation and senescence. (A,B) U2OS cells transfected with pcDNA3-HA encoding WT, L441P and R453C PRODH were subjected to immunoblot analysis (A) and a ROS assay using the ROS-Glo H_2O_2 Assay kit (B; *n*=6 independent cultures). (C,D) U2OS cells overexpressing WT, L441P and R453C PRODH were selected with G418 and treated with 2 µM etoposide, and then subjected to staining for SA-β-Gal (C) and an EdU proliferation assay (D). Data are mean±s.d. Statistical significance was determined using the Student's *t*-test analysis (*n*=3, except in B where *n*=6 independent cultures).

Journal of Cell Science

Journal of Cell Science (2017) 130, 1413-1420 doi:10.1242/jcs.196469

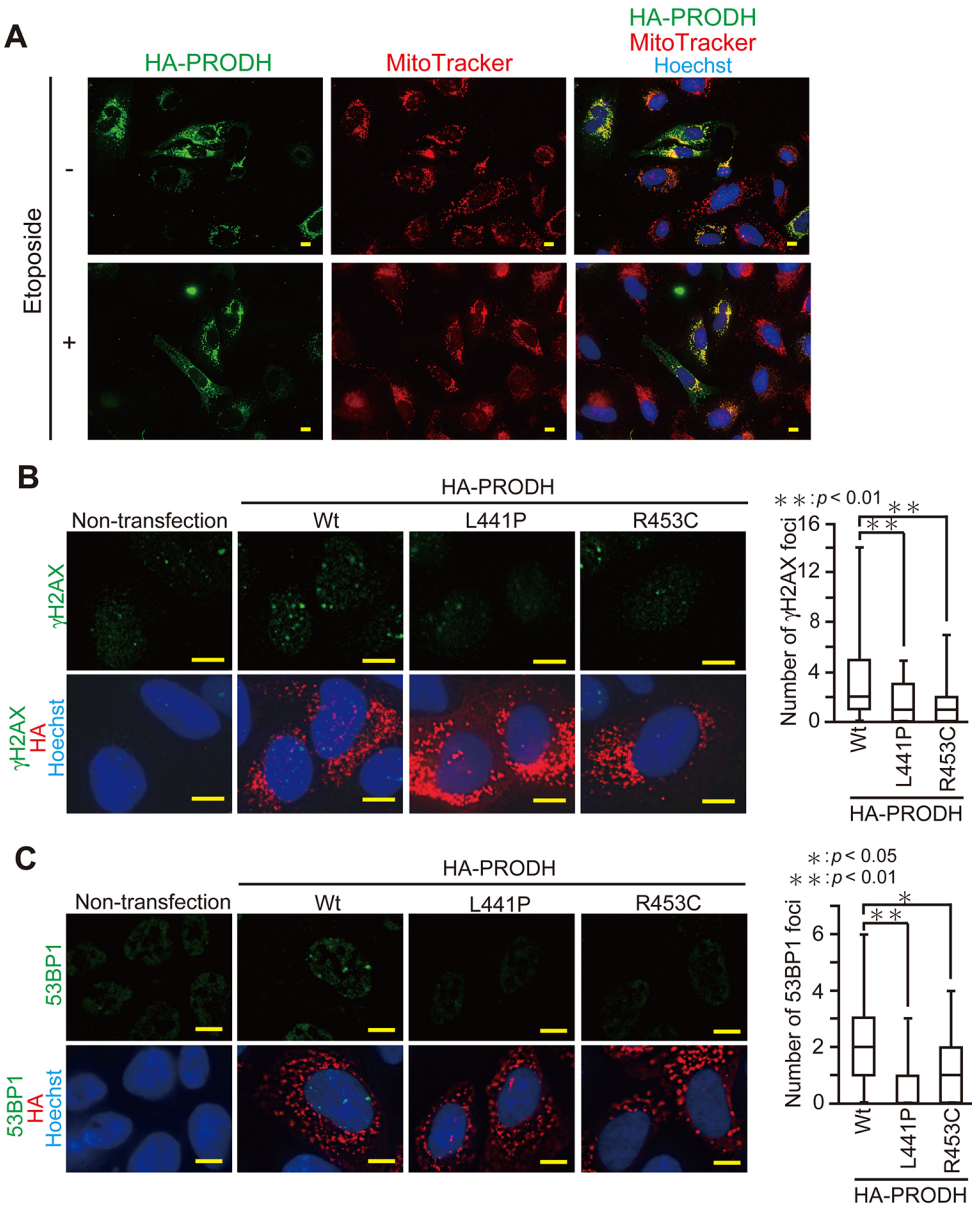

Fig. 5. Overexpression of PRODH causes DNA damage. (A) U2OS cells transfected with pcDNA3-HA-WT-PRODH were treated with 2 µM etoposide for 24 h. The cells were then incubated with 250 nM MitoTracker for 30 min and observed under a fluorescence microscope after immunostaining for HA and Hoechst 33258 staining. Scale bars: 10 µm. (B,C) U2OS cells overexpressing WT, L441P or R453C PRODH were subjected to immunostaining with antibodies against γH2AX (B) or 53BP1 (C) in combination with an antibody against HA. Representative microscope images (left), and box plots of the number of γH2AX and 53BP1 foci in HA–PRODH-expressing cells (right) are shown. The upper and lower limits of the boxes and the lines across the boxes indicate the 75th and 25th percentiles and the median, respectively. Error bars (whiskers) indicate the 90th and 10th percentiles. Non-transfected cells were used as a negative control. Scale bars: 10 µm. Statistical significance was determined using the Student's *t*-test analysis (n=50 cells).

and treatment with NAC, a ROS scavenger, prevented senescence induced by PRODH overexpression. It is widely accepted that ROS contribute to senescence (Campisi, 2013; Salama et al., 2014; Lu and Finkel, 2008). Intracellular ROS levels increase in both replicative and premature senescence, and the treatment of cells with a sublethal dose of H_2O_2 induces senescence (Chen and Ames, 1994). ROS are considered to mediate senescence through induction of DNA damage, and a recent study has reported that a positive-feedback loop between ROS production and the DDR establishes senescence (Passos et al., 2010). Consistent with this, we showed that PRODH overexpression induces DNA damage. Since we have previously revealed that PRODH is upregulated by p53 during senescence (Nagano et al., 2016), these results indicate that PRODH upregulated by p53 in response to senescence-inducing stresses amplifies DNA damage through ROS generation, thereby inducing senescence.

Senescence is now considered to play a critical role in tumor suppression as well as in aging-related disorders in various tissues resulting from the permanent loss of proliferation capacity (Campisi, 2013; Salama et al., 2014). In accordance with the important role of PRODH in senescence, PRODH has been suggested to act as a tumor suppressor *in vitro* and *in vivo*. Overexpression of PRODH suppresses tumorigenesis through induction of cell cycle arrest in a mouse xenograft model (Liu et al., 2009). Furthermore, the protein level of PRODH is reduced in a variety of human tumor tissues (Liu et al., 2009). *PRODH* is located in chromosome 22q11.2, a region that is often deleted in various human tumors, and patients harboring this deletion (DiGeorge/velocardiofacial syndrome) show a higher frequency of malignancy (Zhu et al., 2004; McDonald-McGinn et al., 2006). Given the role of senescence in limiting tumor cell proliferation, the newly identified link between PRODH and senescence provides a new explanation for the mechanism of tumor suppression through PRODH, that is, PRODH inhibits tumor expansion through the induction of senescence rather than apoptosis. At the same time, however, it has been recently reported that P5C reductases, enzymes that convert P5C to proline (namely, the reverse reaction of PRODH-mediated dehydrogenation), are upregulated by the MYC oncogene and enhance tumor cell proliferation through utilization

Journal of Cell Science (2017) 130, 1413-1420 doi:10.1242/jcs.196469

of NADH and NADPH (Liu et al., 2015). These findings, in conjunction with our results, suggest that activation of the proline metabolic pathway does not merely induce ROS accumulation to prevent cell growth but also affects multiple mechanisms to regulate the proliferation of cancer cells.

By contrast, the relationship between PRODH and aging-related disorders has yet to be comprehensively described; only the contribution of PRODH to longevity in the nematode has been studied (Zarse et al., 2012). Studies in mouse models are needed to determine whether PRODH has roles in senescence and aging as well as tumor-suppression *in vivo*. It has also been shown that overexpression of the antioxidant catalase, which is targeted to mitochondria, significantly delays murine age-related cardiac diseases and extends lifespan, which implies that ROS production in mitochondria exacerbates age-related disorders (Schriner et al., 2005). Furthermore, both PRODH-deficient and -overexpressing mouse strains have been described previously and may be useful models for investigating the possible involvement of PRODH in senescence and aging (Gogos et al., 1999; Stark et al., 2009). Regardless of the outcome of mouse model studies, our results establish a new function of PRODH as an inducer of DNA damage-induced senescence, which may provide new insights into the role of amino acid oxidation in various processes, such as aging and those involved in the development of cancer.

MATERIALS AND METHODS

Cell culture, treatment and transfection

U2OS (a human osteosarcoma line; American Type Culture Collection, Rockville, MD) and Hs68 (normal human diploid fibroblasts; IFO50350, JCRB Cell Bank, Osaka, Japan) (Sayles and Johnson, 1996) cells were cultured in Dulbecco's modified Eagle's medium (DMEM) (Wako, Osaka, Japan) supplemented with 10% fetal bovine serum. For senescence induction, U2OS and Hs68 cells were treated with etoposide (Sigma Aldrich) at 2 and 0.5 µM, respectively, for 48 h and cultured in the medium without the drug for an additional 5 days to develop senescent phenotypes. The concentrations and durations of etoposide necessary to induce senescence have been determined previously (Nakano et al., 2013; Nagano et al., 2016). To inhibit PRODH, the cells were incubated with 5 mM L-THFA (Sigma Aldrich). When NAC (Sigma Aldrich) was used, the cells were incubated with the reagent at 5 mM. Transfection with expression vectors was performed using FuGENE HD (Promega) according to the manufacturer's instructions. The transfectants were selected with 800 µg/ml G418 (Wako) for 5 days where indicated.

RNA interference

ON-TARGETplus Smart Pool siRNA against PRODH (L-009543-00) and its control siRNA (D-001810-10) were from Thermo Scientific Dharmacon. U2OS and Hs68 cells were seeded and transfected with 30 nM of siRNA using HiPerFect Transfection Reagent (Qiagen) according to the manufacturer's instructions.

Antibodies

Anti-PRODH antibody (sc-376401; 1:100), horseradish peroxidase (HRP)-conjugated anti-rat antibody (sc-2032; 1:2500) and alkaline phosphatase (AP)-conjugated anti-rat antibody (sc-2021; 1:2500) were obtained from Santa Cruz Biotechnology; anti-α-tubulin antibody (T9026; 1:1000) and anti-γ-tubulin antibody (T6557; 1:3000) were from Sigma Aldrich; HRP-conjugated anti-mouse antibody (W4021; 1:2500) and AP-conjugated anti-mouse antibody (S3721; 1:7500) were from Promega; anti-HA antibody (1867423; 1:1000) was from Roche; anti-γH2AX antibody (05-636; 1:500) was from Merck Millipore; anti-53BP1 antibody (#4937; 1:100) was from Cell Signaling Technology.

Immunoblot analysis

The cells were lysed in SDS sample buffer (50 mM Tris-HCl, pH 6.8, 2% SDS, 5% 2-mercaptoethanol, 0.1% Bromophenol Blue, 10% glycerol). The lysates were separated by SDS-polyacrylamide gel electrophoresis and blotted onto Immobilon polyvinylidene difluoride membrane (Merck Millipore). Each protein was visualized using primary antibodies, enzyme-conjugated secondary antibodies (HRP or AP) and the ECL detection reagent (GE Healthcare) or the NBT/BCIP substrate (Nacalai Tesque, Kyoto, Japan).

Senescence assays

Detection of SA-β-Gal activity was performed using Senescence β-Galactosidase staining kit (Cell Signaling Technology) according to the manufacturer's instructions. Briefly, the cells were fixed with 2% formaldehyde and 0.2% glutaraldehyde. After incubation with SA-β-Gal staining solution (1 mg/ml 5-bromo-4-chloro-3-indolyl-β-D-galactoside, 40 mM citric acid with sodium phosphate [pH 6.0], 5 mM potassium ferrocyanide, 5 mM potassium ferricyanide, 150 mM NaCl, 2 mM $MgCl_2$) for 24 h, the cells were examined under a fluorescence microscope (model BZ-8000; Keyence, Osaka, Japan). At least 100 cells in randomly selected microscope fields were counted to determine the percentage of SA-β-Gal-positive cells. For the EdU incorporation assay, cells were labeled with 10 µM EdU (Life Technologies) for 3 h (U2OS cells) or 24 h (Hs68 cells). Detection of EdU incorporation into the DNA was performed with a Click-iT EdU Imaging Kit (Life Technologies) according to the manufacturer's instructions. After staining nuclei with 10 µM Hoechst 33342, cells were examined under a fluorescence microscope (model BZ-9000; Keyence).

RNA isolation and semi-quantitative RT-PCR

Total RNA was isolated using RNeasy Mini kit (Qiagen) according to the manufacturer's instructions, and cDNAs were generated using ReverTraAce qPCR RT Master Mix with gDNA Remover (TOYOBO, Osaka, Japan). The resulting cDNAs were subjected to PCR amplification using specific primers for *PRODH* (a forward primer: 5′-CATCGAAGCCTCAGGTAG-AGT-3′ and a reverse primer: 5′-CCCCAGTGCTGTGAGCTTAAT-3′) and *GAPDH* (a forward primer: 5′-CAATGACCCCTTCATTGACCT-3′ and a reverse primer: 5′-ATGACAAGCTTCCCGTTCTC-3′). The PCR products were separated by electrophoresis on a 2% agarose gel and detected by ethidium bromide staining.

Plasmid constructions

For construction of pcDNA3-HA-PRODH, an expression vector of HA-tagged human full-length *PRODH* (NCBI accession number NM_016335.4), the PRODH cDNA was amplified with a pair of primers (a forward primer: 5′-GCGAATTCACCATGGCTCTGAGGCGCGC-3′ and a reverse primer: 5′-CGTCTCGAGCTAGGCAGGGCGATGGAAG-3′) using a cDNA sample prepared from U2OS cells as a template. The resulting fragment was digested with EcoRI and XhoI, and cloned downstream of the HA tag sequence into the pcDNA3-HA vector (Invitrogen). To generate PRODH mutants (L441P and R453C), PCR reactions were performed using mutagenic primers (a forward primer: 5′-GGTGTTTTGGGGCCAAGCC-CGTGCGGGGCGCATACCTG-3′ and a reverse primer: 5′-CAGGTAT-GCGCCCCGCACGGGCTTGGCCCCAAAACACC-3′ for L441P; and a forward primer: 5′-GCATACCTGGCCCAGGAGCGAGCCTGTGCGG-CAGAGATCG-3′ and a reverse primer: 5′-CGATCTCTGCCGCACAG-GCTCGCTCCTGGGCCAGGTATGC-3′ for R453C).

Apoptosis assay

The Annexin-V-FLUOS Staining Kit (Roche) was used to detect apoptotic cells. The cells were harvested and resuspended in Annexin-V-FLUOS buffer, and the stained cells were observed under a fluorescence microscope (model BZ-9000; Keyence).

ROS assay

ROS levels were determined by using the ROS-Glo H_2O_2 Assay kit (Promega) and CM-H_2DCFDA (Life Technologies) following the manufacturers' protocols. For ROS-Glo H_2O_2 staining, the cells were incubated at 37°C for 3 h in DMEM containing 25 µM of H_2O_2 substrate that reacts with H_2O_2 to generate a luciferin precursor. Afterwards, ROS-Glo Detection Solution containing recombinant luciferase was added to the

medium, and luminescence was measured using a Mithras LB940 luminometer (Berthold, Bad Wildbad, Germany). For CM-H_2DCFDA staining, cells were stained with 1 µM CM-H_2DCFDA for 10 min at 37°C and trypsinized, and the fluorescence was measured using a BD Accuri C6 flow cytometer (BD Biosciences).

Immunofluorescence

For immunofluorescence analysis, the cells were fixed with 4% paraformaldehyde, permeabilized in 0.5% Triton X-100 and then incubated with primary antibodies in Can Get Signal immunostain Solution B (TOYOBO) overnight at 4°C followed by incubation with Alexa-Fluor-488-conjugated secondary antibodies (Life Technologies) for 1 h at room temperature. After staining cell nuclei with Hoechst 33258, the cells were examined under a fluorescence microscope (model BZ-9000; Keyence). For mitochondria staining, the cells were incubated with 250 nM MitoTracker Red CMXRos (Life Technologies) for 30 min before fixation.

Competing interests

The authors declare no competing or financial interests.

Author contributions

S.K. conceived and designed the experiments. T.N., K.O., K.K., Y.A., M.K. and S.K. performed the experiments. T.N., A.N., K.O., T.I. and S.K. analyzed the data. T.N., A.N., K.O., T.I., U.K. and S.K. contributed reagents/materials/analysis tools. T.N. and S.K. wrote the manuscript.

Funding

This work was supported by Japan Society for the Promotion of Science KAKENHI grant number 25640063.

References

Aksoy, O., Chicas, A., Zeng, T., Zhao, Z., McCurrach, M., Wang, X. and Lowe, S. W. (2012). The atypical E2F family member E2F7 couples the p53 and RB pathways during cellular senescence. *Genes Dev.*. **26**, 1546-1557.

Bender, H.-U., Almashanu, S., Steel, G., Hu, C.-A., Lin, W.-W., Willis, A., Pulver, A. and Valle, D. (2005). Functional consequences of PRODH missense mutations. *Am. J. Hum. Genet.* **76**, 409-420.

Brady, C. A., Jiang, D., Mello, S. S., Johnson, T. M., Jarvis, L. A., Kozak, M. M., Kenzelmann Broz, D., Basak, S., Park, E. J., McLaughlin, M. E. et al. (2011). Distinct p53 transcriptional programs dictate acute DNA-damage responses and tumor suppression. *Cell* **145**, 571-583.

Campisi, J. (2013). Aging, cellular senescence, and cancer. *Annu. Rev. Physiol.* **75**, 685-705.

Carvajal, L. A., Hamard, P.-J., Tonnessen, C. and Manfredi, J. J. (2012). E2F7, a novel target, is up-regulated by p53 and mediates DNA damage-dependent transcriptional repression. *Genes Dev.*. **26**, 1533-1545.

Chen, Q. and Ames, B. N. (1994). Senescence-like growth arrest induced by hydrogen peroxide in human diploid fibroblast F65 cells. *Proc. Natl. Acad. Sci. USA* **91**, 4130-4134.

d'Adda di Fagagna, F. (2008). Living on a break: cellular senescence as a DNA-damage response. *Nat. Rev. Cancer* **8**, 512-522.

Di Leonardo, A., Linke, S. P., Clarkin, K. and Wahl, G. M. (1994). DNA damage triggers a prolonged p53-dependent G1 arrest and long-term induction of Cip1 in normal human fibroblasts. *Genes Dev.*. **8**, 2540-2551.

Dimri, G. P., Lee, X., Basile, G., Acosta, M., Scott, G., Roskelley, C., Medrano, E. E., Linskens, M., Rubelj, I., Pereira-Smith, O. et al. (1995). A biomarker that identifies senescent human cells in culture and in aging skin in vivo. *Proc. Natl. Acad. Sci. USA* **92**, 9363-9367.

Donald, S. P., Sun, X. Y., Hu, C. A., Yu, J., Mei, J. M., Valle, D. and Phang, J. M. (2001). Proline oxidase, encoded by p53-induced gene-6, catalyzes the generation of proline-dependent reactive oxygen species. *Cancer Res.*. **61**, 1810-1815.

el-Deiry, W. S., Tokino, T., Velculescu, V. E., Levy, D. B., Parsons, R., Trent, J. M., Lin, D., Mercer, W. E., Kinzler, K. W. and Vogelstein, B. (1993). WAF1, a potential mediator of p53 tumor suppression. *Cell* **75**, 817-825.

Gogos, J. A., Santha, M., Takacs, Z., Beck, K. D., Luine, V., Lucas, L. R., Nadler, J. V. and Karayiorgou, M. (1999). The gene encoding proline dehydrogenase modulates sensorimotor gating in mice. *Nat. Genet.* **21**, 434-439.

Hu, C.-A., Donald, S. P., Yu, J., Lin, W.-W., Liu, Z., Steel, G., Obie, C., Valle, D. and Phang, J. M. (2007). Overexpression of proline oxidase induces proline-dependent and mitochondria-mediated apoptosis. *Mol. Cell. Biochem.* **295**, 85-92.

Kuilman, T., Michaloglou, C., Mooi, W. J. and Peeper, D. S. (2010). The essence of senescence. *Genes Dev.*. **24**, 2463-2479.

Liu, Y., Borchert, G. L., Donald, S. P., Diwan, B. A., Anver, M. and Phang, J. M. (2009). Proline oxidase functions as a mitochondrial tumor suppressor in human cancers. *Cancer Res.*. **69**, 6414-6422.

Liu, W., Hancock, C. N., Fischer, J. W., Harman, M. and Phang, J. M. (2015). Proline biosynthesis augments tumor cell growth and aerobic glycolysis: involvement of pyridine nucleotides. *Sci. Rep.* **5**, 17206.

Lu, T. and Finkel, T. (2008). Free radicals and senescence. *Exp. Cell Res.* **314**, 1918-1922.

McDonald-McGinn, D. M., Reilly, A., Wallgren-Pettersson, C., Hoyme, H. E., Yang, S. P., Adam, M. P., Zackai, E. H. and Sullivan, K. E. (2006). Malignancy in chromosome 22q11.2 deletion syndrome (DiGeorge syndrome/velocardiofacial syndrome). *Am. J. Med. Genet. A* **140A**, 906-909.

Nagano, T., Nakano, M., Nakashima, A., Onishi, K., Yamao, S., Enari, M., Kikkawa, U. and Kamada, S. (2016). Identification of cellular senescence-specific genes by comparative transcriptomics. *Sci. Rep.* **6**, 31758.

Nakano, M., Nakashima, A., Nagano, T., Ishikawa, S., Kikkawa, U. and Kamada, S. (2013). Branched-chain amino acids enhance premature senescence through mammalian target of rapamycin complex I-mediated upregulation of p21 protein. *PLoS ONE* **8**, e80411.

Noda, A., Ning, Y., Venable, S. F., Pereira-Smith, O. M. and Smith, J. R. (1994). Cloning of senescent cell-derived inhibitors of DNA synthesis using an expression screen. *Exp. Cell Res.* **211**, 90-98.

Passos, J. F., Nelson, G., Wang, C., Richter, T., Simillion, C., Proctor, C. J., Miwa, S., Olijslagers, S., Hallinan, J., Wipat, A. et al. (2010). Feedback between p21 and reactive oxygen production is necessary for cell senescence. *Mol. Syst. Biol.* **6**, 347.

Phang, J. M., Donald, S. P., Pandhare, J. and Liu, Y. (2008). The metabolism of proline, a stress substrate, modulates carcinogenic pathways. *Amino Acids* **35**, 681-690.

Polyak, K., Xia, Y., Zweier, J. L., Kinzler, K. W. and Vogelstein, B. (1997). A model for p53-induced apoptosis. *Nature* **389**, 300-305.

Raimondi, I., Ciribilli, Y., Monti, P., Bisio, A., Pollegioni, L., Fronza, G., Inga, A. and Campomenosi, P. (2013). P53 family members modulate the expression of PRODH, but not PRODH2, via intronic p53 response elements. *PLoS ONE* **8**, e69152.

Rogakou, E. P., Boon, C., Redon, C. and Bonner, W. M. (1999). Megabase chromatin domains involved in DNA double-strand breaks in vivo. *J. Cell Biol.* **146**, 905-916.

Romanov, V. S., Pospelov, V. A. and Pospelova, T. V. (2012). Cyclin-dependent kinase inhibitor p21(Waf1): contemporary view on its role in senescence and oncogenesis. *Biochemistry (Mosc.)* **77**, 575-584.

Rufini, A., Tucci, P., Celardo, I. and Melino, G. (2013). Senescence and aging: the critical roles of p53. *Oncogene* **32**, 5129-5143.

Salama, R., Sadaie, M., Hoare, M. and Narita, M. (2014). Cellular senescence and its effector programs. *Genes Dev.*. **28**, 99-114.

Sayles, P. C. and Johnson, L. L. (1996). Intact immune defenses are required for mice to resist the ts-4 vaccine strain of Toxoplasma gondii. *Infect. Immun.* **64**, 3088-3092.

Schriner, S. E., Linford, N. J., Martin, G. M., Treuting, P., Ogburn, C. E., Emond, M., Coskun, P. E., Ladiges, W., Wolf, N., Van Remmen, H. et al. (2005). Extension of murine life span by overexpression of catalase targeted to mitochondria. *Science* **308**, 1909-1911.

Schultz, L. B., Chehab, N. H., Malikzay, A. and Halazonetis, T. D. (2000). p53 binding protein 1 (53BP1) is an early participant in the cellular response to DNA double-strand breaks. *J. Cell Biol.* **151**, 1381-1390.

Serrano, M., Lin, A. W., McCurrach, M. E., Beach, D. and Lowe, S. W. (1997). Oncogenic ras provokes premature cell senescence associated with accumulation of p53 and p16INK4a. *Cell* **88**, 593-602.

Stark, K. L., Burt, R. A., Gogos, J. A. and Karayiorgou, M. (2009). Analysis of prepulse inhibition in mouse lines overexpressing 22q11.2 orthologues. *Int. J. Neuropsychopharmacol.* **12**, 983-989.

Tallarita, E., Pollegioni, L., Servi, S. and Molla, G. (2012). Expression in Escherichia coli of the catalytic domain of human proline oxidase. *Protein Expr. Purif.* **82**, 345-351.

te Poele, R. H., Okorokov, A. L., Jardine, L., Cummings, J. and Joel, S. P. (2002). DNA damage is able to induce senescence in tumor cells *in vitro* and *in vivo*. *Cancer Res.*. **62**, 1876-1883.

Valente, L. J., Gray, D. H. D., Michalak, E. M., Pinon-Hofbauer, J., Egle, A., Scott, C. L., Janic, A. and Strasser, A. (2013). p53 efficiently suppresses tumor development in the complete absence of its cell-cycle inhibitory and proapoptotic effectors p21, Puma, and Noxa. *Cell Rep.* **3**, 1339-1345.

Vousden, K. H. and Prives, C. (2009). Blinded by the light: the growing complexity of p53. *Cell* **137**, 413-431.

Walker, P. R., Smith, C., Youdale, T., Leblanc, J., Whitfield, J. F. and Sikorska, M. (1991). Topoisomerase II-reactive chemotherapeutic drugs induce apoptosis in thymocytes. *Cancer Res.*. **51**, 1078-1085.

Zarse, K., Schmeisser, S., Groth, M., Priebe, S., Beuster, G., Kuhlow, D., Guthke, R., Platzer, M., Kahn, C. R. and Ristow, M. (2012). Impaired insulin/IGF1 signaling extends life span by promoting mitochondrial L-proline catabolism to induce a transient ROS signal. *Cell Metab.*. **15**, 451-465.

Zhu, G.-N., Zuo, L., Zhou, Q., Zhang, S. M., Zhu, H. Q., Gui, S. Y. and Wang, Y. (2004). Loss of heterozygosity on chromosome 10q22-10q23 and 22q11.2-22q12.1 and p53 gene in primary hepatocellular carcinoma. *World J. Gastroenterol.* **10**, 1975-1978.